Ordered Crystalline Alumina Molecular Sieves Synthesized via a Nanocasting Route

Qian Liu,[†,‡] Aiqin Wang,[†] Xiaodong Wang,[†] and Tao Zhang*[,†]

State Key Laboratory of Catalysis, Dalian Institute of Chemical Physics, Chinese Academy of Sciences, Dalian 116023, People's Republic of China, and Graduate School of the Chinese Academy of Sciences, Beijing 100049, People's Republic of China

Received July 10, 2006
Revised Manuscript Received September 25, 2006

Since the discovery of ordered mesoporous silica (OMS),[1,2] due to the great potentials of alumina in catalysis, adsorption, and separation, many attempts have been made to synthesize ordered mesoporous alumina (OMA) following similar pathways to OMS.[3,4] However, few attempts have been successful,[5,6] and in most cases only disordered channels were produced. This may be ascribed to its susceptibility for hydrolysis, as well as to phase transitions accompanying the thermal breakdown of the ordered structure, thus rendering great difficulties for creating ordered mesopores after the removal of the surfactants. Very recently, Niesz et al. have first reported the synthesis of OMA through precise control of the hydrolysis and condensation of the precursor.[5] However, their OMA displayed lower long-range order compared with OMS and consisted of amorphous framework walls, which limited greatly its applications.[7,8] It has been reported that for the so-called "soft" surfactant templating route, the constraints associated with a crystalline structure cannot be easily accommodated by the large curvature of the mesopores.[9] Consequently, OMA with crystalline framework walls has not been obtained so far.

Not long ago, a nanocasting route using OMS as "hard" templates has been developed to prepare nonsiliceous mesoporous materials.[10,11] Compared with the conventional surfactant templates, the hard templates possess stable topological structures, which would not be disturbed by the synthesis variations and meanwhile could effectively sustain the local strain caused by the crystallization of precursors and thus result in the products being the precise inverse replication of templates.[12−14] Such a nanocasting strategy overcomes the disadvantages of the soft-templating method and therefore provides new opportunities for preparing the unobtainable nonsiliceous ordered mesoporous materials.[15−18] However, though this strategy is conceptually straightforward, it still remains an experimental challege, and many replicas display disordered structures owing to partial loadings of precursors inside mesopores and fast growth outside the mesopores.[19,20]

Scheme 1. Schematic Representation of the Nanocasting Procedure for OCAMS-1 Synthesis[a]

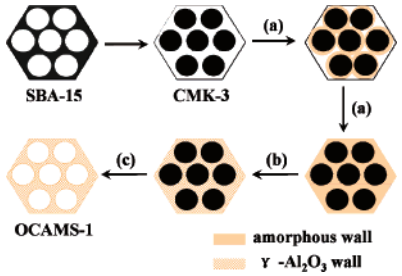

[a] (a) In situ filling of CMK-3 pores with aluminum hydroxide; (b) transformation from amorphous aluminum hydroxide to the crystalline γ-Al_2O_3 phase by calcination in an inert atmosphere; and (c) removal of the carbon template by calcination in air.

In this paper, we describe for the first time the synthesis of ordered crystalline alumina molecular sieves (denoted as OCAMS-1) through rationally designing a repeated nanocasting route and exquisitely controlling the experimental procedure. A highly ordered mesoporous carbon CMK-3 replicated from SBA-15 was used as the rigid template. The product OCAMS-1 displayed highly ordered hexagonal mesopores similar to that of its original template SBA-15 and crystalline γ-Al_2O_3 framework walls.

It is known that an accurate control of the interaction between an inorganic precursor and a hard template is very important for nanocasting synthesis. To obtain a good infusion and filling of the aluminum precursor into CMK-3 mesopores, an ethanol solution of aluminum nitrate was chosen as the precursor. The choice of ethanol as a solvent can improve the wettability of CMK-3 to a certain extent and thus facilitate a uniform loading of aluminum nitrate into pores. The synthesis strategy is illustrated in Scheme 1.

* To whom correspondance should be addressed. Tel.: +86 411 8437 9015. Fax: +86 411 8469 1570. E-mail: taozhang@dicp.ac.cn.
[†] DICP.
[‡] Graduate school of CAS.

(1) Kresge, C. T.; Leonowicz, M. E.; Roth, W. J.; Vartuli, J. C.; Beck, J. S. *Nature* **1992**, *359*, 710.
(2) Zhao, D.; Feng, J.; Huo, Q.; Melosh, N.; Fredrickson, G. H.; Chmelka, B. F.; Stucky, G. D. *Science* **1998**, *279*, 548.
(3) Čejka, J. *Appl. Catal. A* **2003**, *254*, 327 and references therein.
(4) Tian, B.; Liu, X.; Tu, B.; Yu, C.; Fan, J.; Wang, L.; Xie, S.; Stucky, G. D.; Zhao, D. *Nat. Mater.* **2003**, *2*, 159.
(5) Niesz, K.; Yang, P.; Somorjai, G. A. *Chem. Commun.* **2005**, 1986.
(6) Kuemmel, M.; Grosso, D.; Boissière, C.; Smarsly, B.; Brezesinski, T.; Albouy, P. A.; Amenitsch, H.; Sanchez, C. *Angew. Chem., Int. Ed.* **2005**, *44*, 4589.
(7) Zhang, Z.; Hicks, R. W.; Pauly, T. R.; Pinnavaia, T. J. *J. Am. Chem. Soc.* **2002**, *124*, 1592.
(8) Liu, Q.; Wang, A.; Wang, X.; Zhang, T. *Microporous Mesoporous Mater.* **2006**, *92*, 10.
(9) Schüth, F. *Chem. Mater.* **2001**, *13*, 3184.
(10) Ryoo, R.; Joo, S. H.; Jun, S. *J. Phys. Chem. B* **1999**, *103*, 7743.
(11) Jun, S.; Joo, S. H.; Ryoo, R.; Kruk, M.; Jaroniec, M.; Liu, Z.; Ohsuna, T.; Terasaki, O. *J. Am. Chem. Soc.* **2000**, *122*, 10712.
(12) Kang, M.; Yi, S. H.; Lee, H. I.; Yie, J. E.; Kim, J. M. *Chem. Commun.* **2002**, 1944.
(13) Lu, A.; Schmidt, W.; Taguchi, A.; Spliethoff, B.; Tesche, B.; Schüth, F. *Angew. Chem., Int. Ed.* **2002**, *41*, 3489.
(14) Dong, A.; Ren, N.; Tang, Y.; Wang, Y.; Zhang, Y.; Hua, W.; Gao, Z. *J. Am. Chem. Soc.* **2003**, *125*, 4976.
(15) Katou, T.; Lee, B.; Lu, D.; Kondo, J. N.; Hara, M.; Domen, K. *Angew. Chem., Int. Ed.* **2003**, *42*, 2382.
(16) Roggenbuck, J.; Tiemann, M. *J. Am. Chem. Soc.* **2005**, *127*, 1096.
(17) Jiao, F.; Harrison, A.; Jumas, J.-C.; Chadwick, A. V.; Kockelmann, W.; Bruce, P. G. *J. Am. Chem. Soc.* **2006**, *128*, 5468.
(18) Dickinson, C.; Zhou, W.; Hodgkins, R. P.; Shi, Y. F.; Zhao, D. Y.; He, H. Y. *Chem. Mater.* **2006**, *18*, 3088.
(19) Schüth, F. *Angew. Chem., Int. Ed.* **2003**, *42*, 3604.
(20) Wan, Y.; Yang, H.; Zhao, D. Y. *Acc. Chem. Res.* **2006**, *39*, 423.

10.1021/cm0615727 CCC: $33.50
Published on Web 10/06/2006

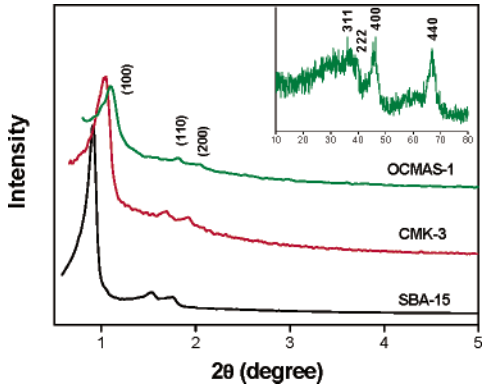

Figure 1. Low-angle XRD patterns for SBA-15, CMK-3, and OCAMS-1 and the wide-angle pattern for OCAMS-1 (inset).

Table 1. Textural Properties of Samples

sample	method	S_{BET} (m^2/g)	V_p (cm^3/g)	D_p[a] (nm)	d_{100} (nm)
SBA-15		698	0.92	6.6	9.8
CMK-3		1094	1.18	4.2	8.4
OCAMS-1	4 times	396	0.46	4.6	8.1
/	2 times	261	0.55	5.9	
/[b]	4 times	257	0.48	6.1	

[a] The mean pore sizes were calculated by applying the BJH method on the desorption branches of the isotherms. [b] The sample was prepared by calcination at 550 °C in air for 3 h.

The CMK-3 template was soaked with the ethanol solution of aluminum nitrate, and then ammonia was filled into the CMK-3 pores to hydrolyze the aluminum in situ. The filling and hydrolysis steps were repeated at least four times to ensure that the template pores were fully filled with the aluminum precursor. Finally, a stepwise calcination procedure was applied to transform the amorphous framework walls to a crystalline γ-Al_2O_3 structure under an inert atmosphere and to remove subsequently the carbon template in air.

Figure 1 presents typical X-ray diffraction (XRD) patterns of OCAMS-1, together with those of SBA-15 and CMK-3 which were used consecutively as the templates. In the low-angle region, all the samples show typical reflections of a two-dimensional hexagonal mesostructure with the space group *p6mm*.[2,11] The gradual broadening of the (100) reflection peak with replication times may imply that there is some decrease in the structure order after the repeated nanocasting synthesis. Besides, from the original SBA-15 template to CMK-3 and then to the final alumina replica, the d_{100} distances calculated using the Bragg equation gradually decreased from 9.8 to 8.1 nm (listed in Table 1). Such a difference may be related to structural shrinkage during the carbonization process as well as to the dehydroxylation from aluminum hydroxide to alumina. As the inset in Figure 1 shows, the wide-angle XRD pattern of OCAMS-1 shows four weak diffraction peaks in accordance with the γ-Al_2O_3 phase (JCPDS card no. 10-0425), confirming the presence of crystalline framework walls in OCAMS-1. The mean crystal domain size is estimated to be 5.1 nm by applying the Scherrer equation to the strongest (440) diffraction peak. On the other hand, the pore wall thickness is about 4.7 nm by calculation from the XRD and nitrogen physisorption results (see below). Considering the limited accuracy of the Scherrer equation, this value is consistent

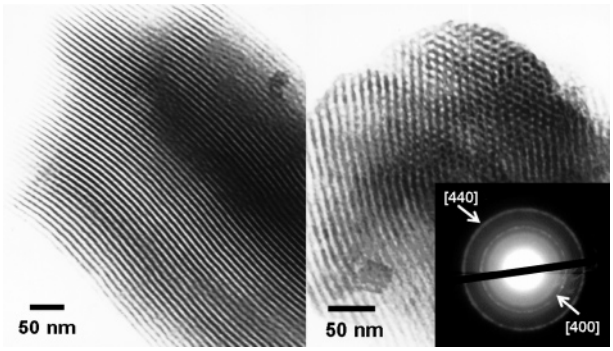

Figure 2. TEM and SAED (inset) images of OCAMS-1.

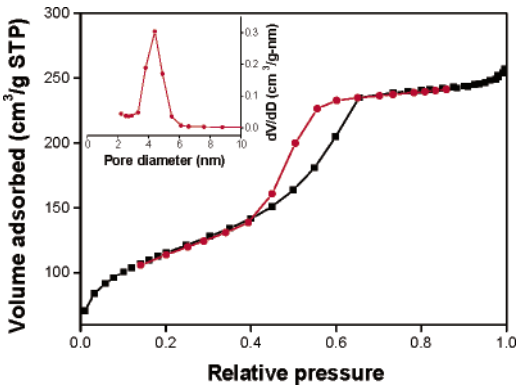

Figure 3. N_2 phsisorption isotherms and corresponding pore size distributions for OCAMS-1.

with the wall thickness of OCAMS-1, again confirming the crystalline framework walls.

The periodic ordered channels of OCAMS-1 can further be observed visually from the representative transmission electron microscopy (TEM) images given in Figure 2. Both the hexagonally ordered mesopores and the evenly spaced parallel channels can clearly be seen, indicating a well-developed long-range order consistent with the XRD results. The selected area electron diffraction (SAED) from the same part of the sample is shown in the inset in Figure 2. It presents concentric diffraction ring patterns, corresponding to the strongest (440) and (400) diffraction of γ-Al_2O_3. Moreover, if the as-synthesized sample was calcined first in N_2 at 750 °C and then in air at 550 °C, the crystallinity can be further increased, as confirmed by the clearly resolved spots on the diffraction rings of the SAED pattern as well as the higher intensities of the XRD peaks (see Supporting information), although the ordering mesostructure was significantly destroyed by such thermal treatment at a higher temperature. Anyway, the above TEM images combined with the SAED pattern further verify that the ordered mesostructures of OCAMS-1 are composed of crystalline γ-Al_2O_3 nanoparticles.[6]

Typical nitrogen adsorption−desorption isotherms and pore size distributions of the obtained alumina samples are shown in Figure 3. The isotherm of OCAMS-1 is characteristic of a type IV isotherm, being similar to those of the original templates of SBA-15 and CMK-3.[2,11] The pore sizes distribution is highly centered at 4.6 nm (Figure 3, inset), much narrower than that reported by Niesz et al.[5] Evidently, our N_2 adsorption−desorption results confirmed again the formation of a long-range ordered mesoporous structure. The

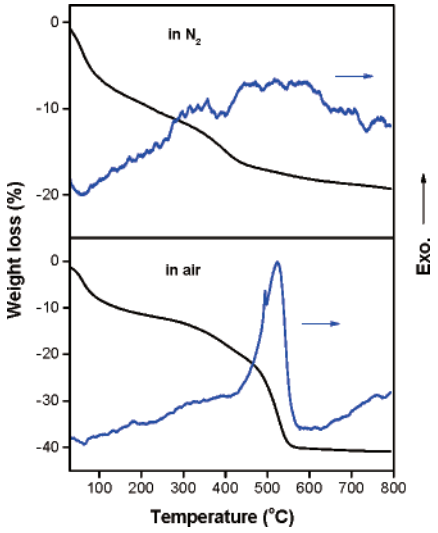

Figure 4. TG-DTA profiles for the as-synthesized samples.

textural parameters of OCAMS-1 and its "parent" SBA-15 and CMK-3 are summarized in Table 1. Compared with SBA-15 and CMK-3, our alumina replica has lower surface area (396 m^2/g) and pore volume (0.46 cm^3/g), which is consistent with the fact that γ-Al_2O_3 has higher density (~3.3 g/cm^3) than those of amorphous silica (~2.2 g/cm^3) and carbon (~1.8 g/cm^3).[7,16]

It was found that the amount of aluminum hydroxide filling into CMK-3 pores and the removal procedure of the carbon template are the two key factors affecting the formation of OCAMS-1. For example, when the filling procedure was repeated only two times, the obtained sample exhibited a quite different isotherm with a wide pore size distribution. Moreover, no discernible peaks appeared in its low angle XRD pattern, and only a disordered wormlike pore system can be observed in the TEM images. These results indicated that the thin inorganic framework walls formed from two aluminum hydroxide precipitations were not strong enough to sustain the ordered mesophase, so that it would collapse upon the template removal process during thermal treatment. Our further experimental results also confirmed that the voids of CMK-3 needed to be filled in situ at least four times for aluminum hydroxide precipitation in order to obtain high-quality OCAMS-1 samples.

On the other hand, even though a high amount of aluminum hydroxide was filled into the CMK-3 pores, an improper carbon template removal procedure would also destroy the ordered mesostructure, resulting in a disordered wormlike pore structure with low surface area, as given in Table 1. Figure 4 compares the thermogravimetric−differential thermal analysis (TG-DTA) profiles of the as-synthesized OCAMS-1 samples under different atmospheres. When the as-synthesized sample was heated in N_2, three weight-loss stages can be observed: removal of physical adsorbed water below 100 °C, dehydration of aluminum hydroxide and transformation to γ-alumina within 100−450 °C, and further crystallization of γ-alumina until 800 °C. It is noted that the thermal effect during the crystallization is continuous and smooth. In contrast, heating the sample in air resulted in a remarkable exothermic effect centered at 520 °C due to combustion of the carbon template. From the TG curve, we can see that the weight loss before 450 °C in N_2 was significantly lower than that in air (17.1% vs 22.3%), indicating carbon combustion in air already occurred before 450 °C, which overlapped with the crystallization of the alumina wall. Thus, the exothermic effect caused by the carbon combustion would destroy the ordered structure of alumina. On the other hand, since the carbon template exhibits high thermal stability under N_2 atmosphere and could be used to preserve the ordered mesoporous structure during the crystallization of framework walls,[21] we first calcined the as-synthesized sample in N_2 to transform the amorphous walls to γ-Al_2O_3 under the protection of a carbon "scaffold" and then removed the carbon template by changing the atmosphere into air at an increased temperature. With such a stepwise-controlled calcination procedure, a highly ordered mesostructure could be well maintained from the preformed thick crystalline framework walls.

In conclusion, a hexagonally ordered crystalline alumina mesoporous molecular sieve OCAMS-1 has been successfully synthesized by a faithfully negative replication of the mesoporous carbon using a rationally designed nanocasting method. An aluminum precursor with modified infiltration properties was filled into the carbon pores and then hydrolyzed in situ, to obtain a stable inorganic framework. The mesoporous carbon not only could act as a rigid template but also could preserve effectively the ordered mesostructure during the crystallization of the amorphous framework walls through a stepwise calcination procedure. Similar strategy can also be expected to be used for preparing other non-siliceous mesoporous materials with both crystalline framework walls and highly ordered mesopores, such as titania, zirconia, and so forth, and even metal carbides.

Acknowledgment. Support of this research by the National Science Foundation of China (NSFC) for Distinguished Young Scholars (No. 20325620) as well as another NSFC grant (No. 20303017) is gratefully acknowledged. We also thank Prof. Liwu Lin, Prof. Dongbai Liang at DICP, and Prof. Dongyuan Zhao at Fudan University for helpful disccussions.

Supporting Information Available: Detailed synthesis procedure and chracterization methods (PDF). This material is available free of charge via the Internet at http://pubs.acs.org.

CM0615727

(21) Katou, T.; Lee, B.; Lu, D.; Kondo, J. N.; Hara, M.; Domen, K. *Angew. Chem., Int. Ed.* **2003**, *42*, 2382.